# Angular distribution of the cosmic ray muon flux at sea-level

Karlo Krakan*
*UBC Department of Physics and Astronomy, Vancouver, Canada*
(Dated: November 25th, 2016)

Accurate measurements of the angular distribution of the cosmic muon flux are important for many applications in science and engineering. In this work, a cosmic muon detector capable of measuring the muon flux at varying zenith angles is used to measure the angular distribution of the muon flux. The resulting data is fit to the $cos^n\theta$ law yielding the fitted shape-parameter $n = 1.84 \pm 0.12$, in agreement with other measurements of this nature.

The muon flux intensity as well as the angular distribution of the muon flux is an important problem in both astrophysics as well as particle physics in general. The muon flux represents a significant source of background radiation for astronomical telescopes and other tools. The exact angular density of the muon flux is important for the calibration of astronomical telescopes, particle detectors, and other sensitive investigative technologies. The muon flux intensity is also an important consideration for sensitive electronics such as processors and solid state devices. Many modern computer processing units are now equipped with software that compensates for the muon flux interference. The muon flux intensity and angular distribution is also important in the determination of the background radiation dose in humans[1] as muons represent the most significant source of cosmic radiation at sea-level. [2]

The cosmic muon flux is also of interest to cosmoclimatology and the study of global warming. In a series of studies, H. Svensmark found that the long-term variation of the cosmic muon flux was found to have a stunningly high correlation with global cloud cover. It has been hypothesized that general historic global warming and cooling trends have been a result of this correlation. [3, 4]

In this work, a pre-existing detector capable of detecting these cosmic muons is used. The shape of the angular distribution is then investigated in two angular regions yielding two differing estimates of the shape parameter. The significance of the two parameters is discussed and a final estimate is determined by a consideration of the angular regions investigated. The shape parameter is found to be consistent with other works of this nature. [8–11] It is of importance to note that the following study was completed at the geographical location 49°15'58.2"N 123°15'07.0"W at about 90m above sea-level as the muon flux intensity and angular distribution may vary slightly between locations on the earth. [5]

The muon flux at sea level is a consequence of cosmic rays, mainly high-energy protons and alpha particles, colliding with particles in the upper atmosphere such as oxygen and nitrogen. These particle collisions produce showers of secondary cosmic rays of muons, pions, photons, neutrons, and other particles. The muons produced by these collisions travel at near light-speed, allowing them to reach sea-level by the effect of time dilation and therefore also allowing for their detection by particle detectors on the ground.

Although muons are not the only particles produced by cosmic ray collisions in the upper atmosphere, other particles produced either have very short mean lifetimes, are absorbed before reaching the surface of the earth, or are just not detectable. The result is that muons are the most abundant secondary cosmic particles at sea level.[2] These muons reach the ground with a mean energy of 4GeV.[2, 6]

It is generally assumed that the angular distribution of the muon flux follows the $cos^n\theta$ law,[1, 7, 8]

$$\frac{dN}{d\Omega dAdt} = I_0 cos^n\theta \tag{1}$$

where $I_0$ is the muon flux intensity with units of cm$^{-2}$ s$^{-1}$ sr$^{-1}$, $n$ is a shape parameter, $A$ is the area of a detector, $\Omega$ is the solid angle of the detector, $\theta$ is the zenith angle, and $N$ is the muon count. Equation (1) is only valid for angles $\theta < 70°$ as angles greater than this are affected by the curvature of the earth and the equation becomes invalid. Experimentally, these parameters have been found to be $I_0 \approx 0.007$cm$^{-2}$ s$^{-1}$ sr$^{-1}$ and $n \approx 2$.[8–11] The muon count rate $\frac{dN}{dt}$ obtained from integration of (1) is dependent on the geometry of a chosen muon detector.

To reduce noise and uncertainty a muon detection technique relying on coincidence is used. Two scintillator paddles and photomultiplier tubes (SP/PMT) combos are positioned parallel to each other with the areas $A_t$ and $A_b$ of either paddle facing the other. The coincidence condition allows for the detection of only the muons that cross both paddles while filtering events corresponding to single events in either scintillator paddle. In this way, muon detection is restricted to only those muons which travel along the zenith-angle orientation (but also within some solid angle about the zenith angle) of the scintillator paddle set-up. Integration of equation (1) takes into account the solid angle of acceptance about the chosen zenith angle.

The scintillator paddles are then housed in a apparatus allowing the two paddles to rotate about the central axis parallel to the orientation of the scintillator paddles. The rotation of the paddles allows for the varying of the zenith angle $\theta$, where $\theta = 0$ corresponds to the angle straight up. This detector set-up has been pre-made,

* karlo@krakan.ca

though processing of the signal from the detector was developed independently and will be explained later.

Integrating equation (1) over the solid angle $d\Omega$ and the area $dA$ of the chosen muon detector geometry, the observed or expected number of muons after a time $t$ is found to be

$$N(\theta, t) = I_0 \cos^n(\theta) \frac{A_t A_b}{R^2} t \tag{2}$$

Where $A_t$ and $A_b$ are the areas of the two scintillators, $R$ is the distance between the scintillators and $t$ is the total time elapsed in seconds, and the other parameters are the same as in equation (1). Equation (2) is obtained using the simplifying assumption that every detector element $dA$ has the same zenith angle $\theta$ and thus the predicted muon count may not match with the observed count rate. Furthermore, in practice the muon count will also depend on the efficiency of the detector. In this work, the exact geometry and efficiency of the muon detector is unknown and so at best only a detector-dependent muon flux intensity, $I_d$ with units s$^{-1}$, can be determined. However, the important shape parameter $n$ that describes the angular distribution can still be found with relative accuracy.

The detection of the muons is achieved via the SP/PMT combination, but the raw signal output of the PMTs must be processed in order to collect the data we are interested in. The raw output signal of each SP/PMT is fed into a pair of discriminators which are capable of filtering out the PMT pulses below a certain threshold amplitude. The output of the discriminator is then fed into a coincidence detector, a signal processing module which only sends an output pulse if two input pulses arrive within a certain time window that can be set. Finally, the output of the coincidence module is fed into a multi-channel analyzer (MCA) which sends its output to a computer with software capable of counting the number of pulses received by the MCA over a certain time. A diagram of the apparatus can be seen in Fig. 1.

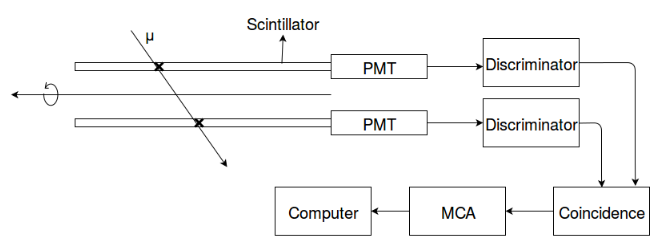


FIG. 1. A diagram of the experimental apparatus. The scintillator paddles are able to swing around the central axis between the paddles allowing for variation in the zenith angle.

The discriminators are set in such a way as to minimize the signals from lower energy particles, such as photons, as well as any intrinsic noise in the SP/PMT combination. This is done by setting the discriminator threshold to an amplitude at a reasonable trade-off between the maximization of the muon signal and minimization of the noise. In this case, the exact threshold amplitude of the discriminators is not known precisely as the mechanism by which to set the threshold on the discriminators used in this work do not allow the threshold to be known precisely. An estimate of the threshold amplitude is ~120mV. The coincidence module time-window is set as low as possible to ensure that only real events are recorded. Since the muons travel at about the speed of light and since the scintillator paddles are about a meter apart, the real muon signal pulses will have a separation of about 3-5ns and so the time window must be set as low as possible in order to not count any events which occur with a larger time separation. In this case, the time window is again not known precisely by nature of the coincidence module used, but has been set at approximately ~6ns. By doing this, it is ensured that the counts collected by the computer are indeed only the counts we are interested in.

In order to measure the angular distribution of the muon flux, the SP/PMTs are rotated through zenith angles between 0° and 90° and set to count muons for 5 hours (18000s) at 10° intervals. The long collection time greatly increases the accuracy of the observed muon counts because counting statistics says that the uncertainty $\delta N$ on any measured number of counts $N$ is $\sqrt{N}$ and therefore the relative uncertainty as a function of $N$ is

$$\frac{\delta N}{N} = \frac{\sqrt{N}}{N} = \frac{1}{\sqrt{N}} \tag{3}$$

meaning that the relative uncertainty of a single measurement decreases as the number counts collected increases.

For a quick check on the validity of the equation (2), the orientation of the detector is set to zenith angle $\theta = 90°$ and set to collect data for some time. There is a very large observed muon count for $\theta = 90°$ whereas (2) implies that $N(\theta = 90°, t) = 0$. The reason for this, as described earlier, is that equation (2) is only valid for $\theta < 70°$ due to the curvature of the earth. Evidently, the data can not be fit to (2) so instead the data is fit to the equation

$$N(\theta, t = T_c) = I_d \cos^n(\theta) T_c + bT_c \tag{4}$$

Where $I_d$ is the detector-dependent muon flux intensity, $T_c$ is the collection time, 18000s in this case, and $b$ is added only to assist in the fit but has unit of s$^{-1}$. The collected data and fit is shown in Fig. 2.

The large number of counts in the data presented in Fig. 2 means that the relative uncertainties in each observation of the muon count are relatively low. In this case, the relative uncertainty of each measurement is below 3.6%. The resulting fitted parameters are $I_d = (5.29 \pm 0.02) \times 10^{-2}$s$^{-1}$, $n = 4.02 \pm 0.33$, and $b = (4.63 \pm 0.01) \times 10^{-2}$s$^{-1}$.

To obtain a better measurement of the detector-dependent muon flux intensity $I_d$ and $n$, the experiment

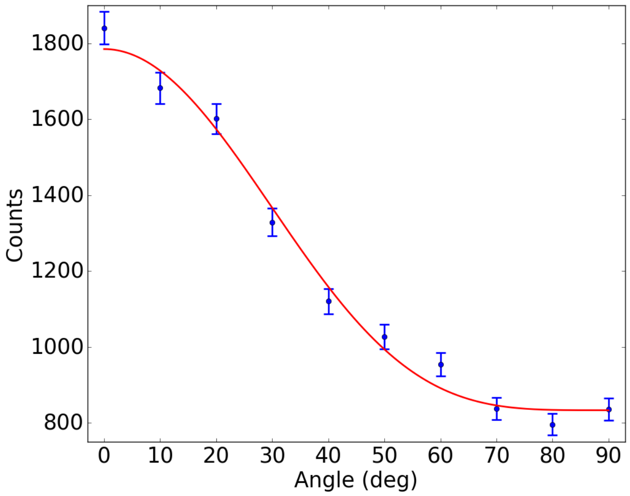


FIG. 2. A plot of the observed muon counts in $10^\circ$ increments between zenith angles $0^\circ$ and $90^\circ$ with collection time $T_c$ = 18000s. The best fit line is shown in red. The data is fit to the equation $N(\theta, t = T_c) = I_d \cos^n(\theta) T_c + bT_c$ where $T_c = 18000s$ The fitted parameters are $I_d = (5.29 \pm 0.02) \times 10^{-2}$s$^{-1}$, $n = 4.02 \pm 0.33$, and $b = (4.63 \pm 0.01) \times 10^{-2}$s$^{-1}$. A $\chi^2$ goodness of fit test reveals $\chi^2 = 12.78$.

is repeated in the angular region where equation (2) most strongly holds, omitting the large angles where (2) does not hold. Now, the apparatus is rotated through $0^\circ$ and $45^\circ$ in $5^\circ$ intervals with a collection time of 1200s. The collected data is shown in Fig. 3.

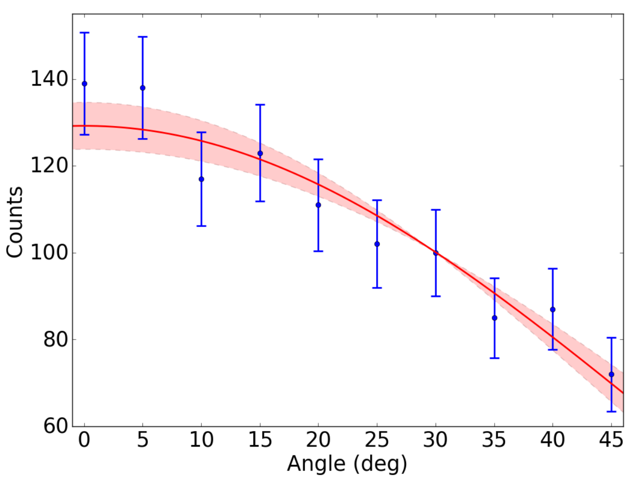


FIG. 3. A plot of the observed muon counts in $5^\circ$ increments between zenith angles $0^\circ$ and $45^\circ$ with collection time $T_c$ = 1200s. The best fit line is shown, the shaded area representing a $1\sigma$ uncertainty on the best fit line. The data is fit to the equation $N(\theta, t = T_c) = I_d \cos^n(\theta) T_c$ where $T_c = 1200s$. The fitted parameters are $I_d = 0.108 \pm 0.005$s$^{-1}$ and $n = 1.77 \pm 0.30$. A $\chi^2$ goodness of fit test reveals $\chi^2 = 3.34$.

Due to time constraints, the muon counts in the data presented above in Fig. 3 are much lower compared to Fig. 2 as only a small collection time was possible (1200s). The result is that relative uncertainties in the above data are much higher, between 9% and 13%. However, the chosen angular region can be fit to (2) (with $I_d$ again replacing $I_0$ and the geometric terms) instead of (4) resulting in a better estimate of the fit parameters, at least in the angular region between $0^\circ$ and $45^\circ$. The fitted parameters are $I_d = 0.104 \pm 0.004$s$^{-1}$ and $n = 1.66 \pm 0.24$.

As explained previously, since the exact detector efficiency and geometry is not known, the detector-dependent muon flux intensity, $I_d$, is not relevant to other works of this nature. On the other hand, the shape parameter, $n$, is relevant and of importance to studies of this nature. This investigation, however, has yielded two differing estimates for this parameter. The first estimate can be ignored, as the obtained data extends beyond the region of applicability of the function being fitted to. The second estimate, $n = 1.66 \pm 0.24$, is a much more useful result. In order to obtain an improved fit, the data between the first trial and second trial are combined and fit the time independent version of equation (2).

$$\frac{dN(\theta)}{dt} = I_d \cos^n(\theta) \tag{5}$$

The uncertainties in the measurements are scaled appropriately according to the collection times. The data is shown in Fig. 4.

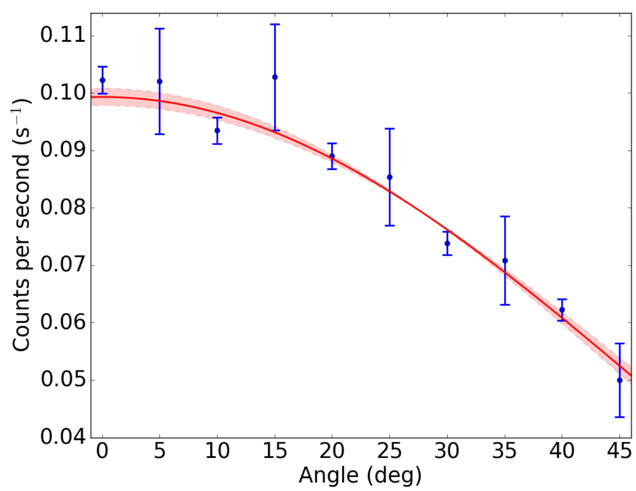


FIG. 4. A plot of the combined muon count data for angles between zenith angles $0^\circ$ and $45^\circ$. The best fit line is shown, the shaded area representing a $1\sigma$ uncertainty on the best fit line. The data is fit to the equation $\frac{dN(\theta)}{dt} = I_d \cos^n(\theta)$. The fitted parameters are $I_d = 0.099 \pm 0.002$s$^{-1}$ and $n = 1.84 \pm 0.12$. A $\chi^2$ goodness of fit test reveals $\chi^2 = 6.91$.

Here, the muon count measurements taken from the first data set are weighted much more strongly due to the smaller uncertainties. When fit to (5) the resulting fitted parameters are $I_d = 0.099 \pm 0.002$s$^{-1}$ and $n = 1.84 \pm 0.12$. The shape parameter $n$ is in good agreement with the previous fit as well as other measurements of this nature. [8–11]

The result for the shape parameter of the angular muon flux distribution, $n = 1.84 \pm 0.12$, determined in this work serves as a confirmation of the years of studies that have been undertaken to describe this phenomena. However, the result in this study has a rather high uncertainty, future works could be undertaken to reduce the uncertainty quoted on this parameter.

A measurement of the muon flux intensity would have also been an important result but unfortunately, due to time constraints, the exact geometry and efficiency of the muon detector was left undetermined. Further work is needed to calculate the muon flux intensity measured in this experiment.


[1] Jeng-Wei Lin, Yen-Fu Chen, Rong-Jiun Sheu, Shiang-Huei Jiang, Nucl. Inst. and Meth. in Phys. Res. A, **619**, Issues 1–3 (2010).
[2] S. Cecchini, M. Spurio, arXiv:1208.1171v1 [astro-ph.EP] (2012).
[3] H. Svensmark, Astr. and Geophys., **48** (1): 1.19, (2007).
[4] H. Svensmark et al, Proceedings of the Royal Society A. 463 (2078): 385-396. (2007).
[5] S. Cecchini, M. Sioli arXiv:hep-ex/0002052v1 (2000).
[6] K Nakamura, et al, J. Phys. G. Nucl. and Part. Phys., **37**, 7A (2010).
[7] T.K. Gaisser, Cosmic Rays and Particle Physics, Cambridge University Press, Cambridge (1990).
[8] P.K.F. Grieder, Cosmic Rays at Earth - Researcher's Reference Manual and Data Book, Elsevier Science, Amsterdam, p. 372 (2001).
[9] Grieder P. K. F., Extensive Air Showers, Springer-Verlag, Berlin, (2010).
[10] T. Kin, K. Chaiwongkhot, H. Ohno, K. Kondo, and Y. Watanabe, JPS Conf. Proc., **11**, 070006 (2016).
[11] A. Dragic, D. Jokovic, R. Banjanac, V. Udovicic, B. Panic, J. Puzovic, I. Anicin, Nucl. Inst. and Meth. in Phys. Res. A, **591**, 3 (2008).